

Semiclassical transport in a square billiard: Conductance oscillations as probe of coherence length

T. Blomquist and I. V. Zozoulenko

Department of Physics (IFM), Linköping University, S-581 83 Linköping, Sweden

(Received 16 September 1999)

We provide a semiclassical interpretation of the conductance oscillations in a square billiard and outline its relation to a commonly used picture of periodic orbits. We demonstrate that the characteristic frequencies in the conductance arise as a result of interference of pairs of long trajectories that typically bounce in a vicinity of the corresponding periodic orbits in the phase space. We present an unambiguous identification of the specific pairs of trajectories causing the pronounced peaks in the observed length spectrum of the conductance. This allows us to extract directly the phase coherence length from the frequency of the observed oscillations.

Statistical properties of the conductance fluctuations originating from the interference of electron waves in submicrometer semiconductor quantum dots (electron billiards) have been a lively area for both experimental and theoretical studies.¹ A second related question is attracting more attention in recent years, namely is it possible to explain/predict the geometry-specific spectrum of the conductance oscillations in a billiard of a given shape (square, circle, stadium etc.).²⁻⁸ One of the most common approaches is based on the Gutzwiller's picture of periodic orbits where the characteristic frequencies of the oscillations in the conductance of open dots are associated with the contribution from simple closed periodic orbits of the corresponding isolated structure²⁻⁶ such that the density of states at the Fermi energy of the isolated dot (broadened due to a finite escape lifetime) dominates fluctuations. Although being intuitively simple and therefore attractive, this picture in fact brushes many important questions under the carpet. For example, the question of how and why the closed orbits (which are often classically decoupled from the leads) mediate conductance is not addressed at all or remains on the level of speculations. However, somehow different predictions may apparently follow from the semiclassical approach where the conductance of the dot arises from the contributions from the all classical trajectories that connect the entrance and the exit leads.^{9,7,8,10} Each of the paths carries an amplitude and a phase. As a result the oscillations are determined by a set of the trajectories relating the billiard leads.

In this paper, we attempt to reconcile these two seemingly different pictures by performing both quantum and semiclassical calculations for the square billiard. The choice of this geometry is motivated by a recent experiment⁵ where the observed frequency of oscillations has remained unexplained as it is a factor of two smaller than that expected from the periodic orbit theory and quantum-mechanical calculations.^{5,6}

In this paper, we demonstrate that, regardless of the lead positions, the several lowest characteristic frequencies in the length spectrum of the conductance oscillations of the open square formally coincides with the length of the shortest periodic orbits. However, we show that these frequencies arise as a result of interference of *pairs of long trajectories* (of the

length of $\sim 3-10L$, L being the square side) which typically bounce in a vicinity of the corresponding periodic orbits in the phase space. The distribution of path differences between these trajectories is often (but not always) peaked at the lengths of the shortest periodic orbits, which explains the observed frequencies.

Introducing a finite coherence length $l_\phi \approx 0.8L$ ($\sim 2 \mu\text{m}$) which suppresses the contribution from long trajectories, we reproduce the experimental result⁵ and thus pinpoint a specific pair of (*short*) trajectories that generated the observed oscillations. This, to the best of our knowledge, represents the first unambiguous identification of the specific frequency of oscillations observed in a billiard of a given shape. Note that the different reports in current literature give estimations of the low temperature l_ϕ ($T \lesssim 0.1$ K) for various billiard systems in a wide range of $0.5-100 \mu\text{m}$.¹¹⁻¹⁴ Moreover, different models of determination of l_ϕ are usually based on rather indirect methods, which, even for the same dot, may give values differing in the order of a magnitude.¹² In contrast, our analysis provides a *direct* determination of the phase coherence length from the characteristic frequencies in the length spectrum, which, in turn, are immediately related to the specific trajectories in the billiard.

Let us consider a square billiard with a pair of ideal leads attached to its opposite sides, see Fig. 1. The zero-temperature conductance of the structure is given by the Landauer formula $G = (2e^2/h)T$ where the total transmission coefficient $T = \sum_{mn} T_{mn}$ is the sum over transmission coefficients from all the propagating modes m in one lead to the modes n in the other; $T_{mn} = |t_{mn}|^2$.¹⁰ In the absence of a magnetic field the transmission amplitude t_{nm} is given by the projection of the retarded Green function onto the transverse wave functions $\phi_n(y)$ in the incoming and outgoing leads⁹

$$t_{mn}(k_F) = -i\hbar \sqrt{v_n v_m} \int dy_1 \int dy_2 \phi_n^*(y_1) \times \phi_m(y_2) G(y_1, y_2, k_F), \quad (1)$$

where v_n is the longitudinal velocity for the mode n and k_F is the Fermi wave vector. We perform both quantum-mechanical and semiclassical calculations of the conduc-

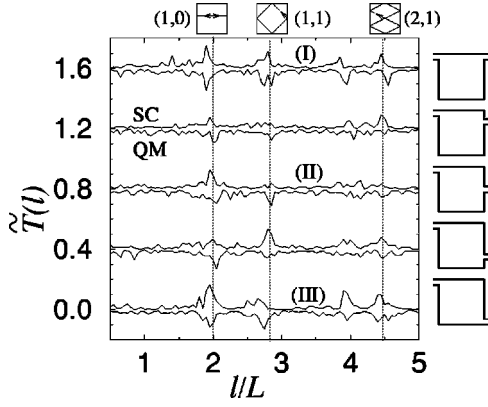


FIG. 1. The length spectrum of the semiclassical (SC) and quantum-mechanical (QM) total transmission coefficient of a square billiard with different lead positions. The QM length spectrum is inverted and curves are shifted for clarity. In the SC calculations the trajectories with up to 10 bounces are included. Here and hereafter the size of the dot is $L=0.72 \mu\text{m}$; $L/w=10$. The F.T. is performed in the interval $1 < k_F w / \pi < 5$. Vertical lines indicate the lengths of the shortest periodic orbits in the closed square, which are schematically depicted in the figure.

tance. In the quantum-mechanical calculations we introduce a tight-binding Hamiltonian and calculate $G(y_1, y_2, k_F)$ using the modified version¹⁵ of the standard recursive Green's-function technique based on the Dyson equation.¹⁰ In the semiclassical treatment we replace the quantum-mechanical Green function by its semiclassical limit.^{9,2} For the square billiard with the hard hard-wall leads of the width w , Eq. (1) reduces to

$$t_{mn}^{sc}(k_F) = \sum_s a_s h_m^*(k_F, \theta_1^s) h_n(k_F, \theta_2^s) e^{ik_F l_s - i\mu_s \pi/2}, \quad (2)$$

where summation is performed over all classical trajectories s connecting the two leads in the square billiard of the size L , l_s being the length of the trajectory and $\theta_{1(2)}^s$ being the corresponding entrance (exit) angles; $a_s = -\sqrt{2k_n k_m / 2\pi i / (w k_F l_s)}$, k_n is the longitudinal wave vector for n th mode, μ_s is the Maslov index, the factor $h_n(k_F, \theta)$ is related to the electron diffraction at the lead mouths and describes an angular distribution of the electrons injected from the lead with the angle θ [an explicit expression for $h_n(k_F, \theta)$ can be found in Ref. 8; see also Ref. 7].

The conductance oscillations are most conveniently analyzed in terms of the length spectrum given by the Fourier transform (F.T.) $\tilde{f}(l) = \int dk_F f(k_F) e^{-ik_F l}$. Because of the rapidly varying phase factor in the exponent in Eq. (2), the spectrum of $\tilde{t}_{nm}(l)$ is strongly peaked at the lengths $l = l_s$ of the classical trajectories connecting the leads (appropriately weighted according to the injection angles and the mode numbers). This behavior of \tilde{t}_{nm} is well understood and verified for a number of different model billiards.^{16,8,7} However, much less attention has been devoted to the analysis of the total transmission coefficient T , which, in contrast to t_{nm} , is accessible experimentally. Figure 1 shows the length spectrum of the total transmission coefficient T of square billiards with different lead positions calculated both quantum mechanically and semiclassically. In the latter, the trajectories

with up to ~ 10 bounces were included in Eq. (2), which is sufficient to achieve a satisfactory agreement with the quantum-mechanical calculations. One of the most remarkable observation is that the oscillation frequencies do not seem to be sensitive to the lead position and the characteristic lengths in the spectrum are typically close to the lengths of the shortest periodic orbits, $l_{(i,j)}^{p.o.} = 2L\sqrt{i^2 + j^2}$, where (i, j) are the positive-integer winding numbers giving the number of collision with one of vertical and one of horizontal boundaries.² To understand this feature let us consider the semiclassical transmission coefficient $T_{nm} = |t_{nm}|^2$

$$T_{mn}^{sc}(k_F) = \sum_s |a_s|^2 |H_s|^2 + \sum_{s,s'} a_s a_{s'}^* H_s H_{s'}^* e^{ik_F(l_s - l_{s'}) - i(\mu_s - \mu_{s'}) \pi/2}, \quad (3)$$

where $H_s = h_m^*(k_F, \theta_1^s) h_n(k_F, \theta_2^s)$. The second term represents a quantum correction to the classical transmission due to interference between paths s and s' . The $\tilde{T}_{nm}^{sc}(l)$ is obviously strongly peaked at the length difference $l = \Delta l \equiv l_s - l_{s'}$ in the pairs of the classical trajectories connecting the leads. Thus, identification of the characteristic frequencies of the oscillations reduces to the analysis of the path difference distribution in a square billiard with a given lead geometry. For this purpose it is convenient to “unfold” a square by reflecting it at all its sides such that each bouncing trajectory transforms into a straight line connecting the original entrance and an unfolded exit, see Fig. 2(b). Each trajectory is characterized by the number of collisions, m and n , with the vertical and the horizontal walls respectively, and the law of Pythagoras immediately gives a trajectory length $l_{m,n}$. A simple analysis shows that the length difference for many pairs of trajectories often converges to the lengths of the shortest periodic orbits of the square. Indeed, consider pairs of trajectories with $m \gg n$, i.e. those where electrons are injected almost parallel to the horizontal boundary such that they bounce in the vicinity of the periodic orbit (1,0) in the phase space. The length difference between two consecutive trajectories is $\Delta l = l_{m+2,n} - l_{m,n} = 2L[1 + O(n/m) + O((d/L)(n/m))]$; d being the distance from the exit to the upper wall. This implies that for all such pairs and regardless of the lead position d , Δl converges to the same value $l_{(1,0)}^{p.o.} = 2L$ provided the trajectories are sufficiently long, $m/n \gg 1$. Similarly, all pairs of long trajectories where electrons are injected close to the diagonal of the square, $m \approx n$ [i.e., in the vicinity of a periodic orbit (1,1)] amount to a length difference $\Delta l \approx l_{(1,1)}^{p.o.} = 2\sqrt{2}L$. It is worth to stress that the characteristic length difference does not always match the length of a periodic orbit. For example, this is the case for the peak in $\tilde{T}(l)$ at $l \approx 4L$ (see Fig. 1), which is caused by pairs of trajectories of the length of $l_{m+4,n}$ and $l_{m,n}$; $m \gg n$.

A detailed inspection of the transmission probability, Eq. (3), supports the analysis performed above. Figure 2 (a) shows $\tilde{T}_{11}(l)$ for a square dot with different lead configurations. Let us concentrate on the peak at $l = 2L$. Figure 2(c) show the pairs of trajectories whose contribution to this peak [calculated according to Eq. (3)] is dominant. As expected, all these trajectories bounce in the vicinity of the periodic

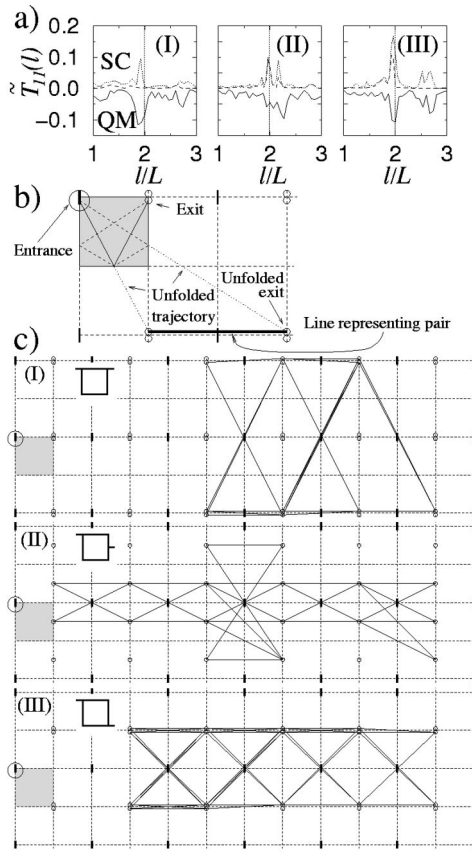


FIG. 2. (a) The length spectrum of the quantum-mechanical (QM) and the semiclassical (SC) transmission coefficient T_{11} for the geometries I–III [see insets in (c) and Fig. 1]. In semiclassical calculations the trajectories with up to 5 and 10 bounces are included (dashed and dotted lines, respectively). The peak at $l = 2L$ is marked by the dotted line. (b) A diagram illustrating the unfolding of bouncing trajectories in a square. An original square (shaded) with a pair of two bouncing trajectories (solid and dashed lines) connecting the entrance and the exit (a fat dash and an open circle respectively). The square is unfolded in a plane by reflecting at all its sides. In this representation each bouncing trajectory in the pair (i.e. the solid and the dashed lines in the shaded square) unfolds into a straight line connecting the entrance (an encircled fat dash in the shaded square) with the corresponding unfolded exit. A solid line connecting the unfolded exits is drawn to identify this pair of trajectories. (c) The solid lines identify the *pairs* of trajectories [as described in (b)] giving a dominant contribution to the peak at $l = 2L$ in (a). The length difference between the trajectories in each pair is $\Delta l \approx 2L$.

orbit (1,0) (i.e. $m \gg n$). [Note that the contribution from the trajectories injected close to the orbit (0,1), i.e. perpendicular to the lead, are suppressed by the angular factor H_s in Eq. (3) which is strongly peaked at $\theta = 0$ for the electrons in the first mode.] Typically, the trajectories must be sufficiently long, $m \geq 4$ in order for their length difference to approach $2L$. However, as evident from Figs. 2(a) and 2(c), the required number of bounces depends on the lead position. For instance, 5 bounces already give a good agreement with the quantum-mechanical calculations for the geometries II and III, whereas for the geometry I this number must be ≥ 8 in

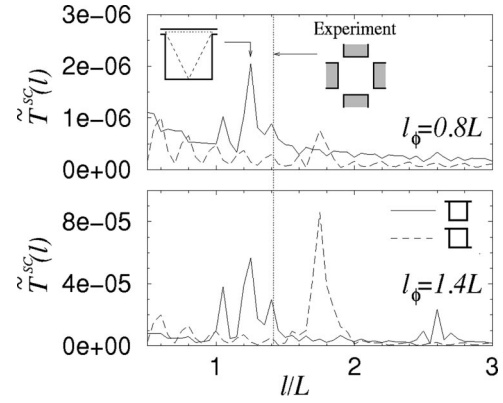


FIG. 3. The length spectrum of the semiclassical total transmission (geometries I and III; solid and dashed lines, respectively) where a finite coherence length is introduced; $l_\phi = 0.8L, 1.4L$. Inset shows the pair of trajectories in the square generating the peak at $l \approx 1.25L$. A vertical line indicates the experimentally observed frequency (Ref. 5) with the corresponding lead geometry.

order to provide the expected contribution to \tilde{T}_{11}^{sc} . Similar analysis for the other modes in the leads and other peaks in the length spectrum can be performed in the same way.

Let us now apply the above analysis to the experiment⁵ where highly periodic oscillations in a square dot at zero field have been observed as a function of k_F with a well-defined single frequency in the length spectrum at $l \approx 1.4L$. The experiment has been performed in a four-terminal geometry with the leads placed at the corners of the square (see inset in Fig. 3). According to the Landauer-Büttiker formalism,¹⁰ the observed four-terminal resistance in this case can be expressed via only two independent transmission coefficients. These coefficients are approximately those given by geometries I and III (Figs. 1 and 2). As shown above, the corresponding calculated length spectra of $\tilde{T}(l)$ are dominated by the pronounced features at $l = 2L, 2\sqrt{2}L$, which are due to relatively long trajectories with $l_s \geq 5 - 7L$. The absence of these frequencies in the experimental spectrum suggests that the above lengths exceed the phase coherent length l_ϕ . In the presence of phase-breaking events the probability that an electron travels the path l_s without losing its phase is $\exp(-l_s/l_\phi)$.¹³ We introduce this probability in Eq. (3) and effectively suppress contributions from the long trajectories. Figure 3 shows that with a reduction of the coherence length $l_\phi \lesssim 0.8L$, only one single frequency $l \approx 1.24L$ survives in the length spectrum. The pair of the shortest trajectories in the square (with the length difference $\sqrt{5}L - L \approx 1.24L$), which cause these oscillations is shown in the inset. The obtained frequency matches the experimentally observed one within the accuracy of 12%, which is satisfactory taking into account the uncertainty in the actual dot dimension etc. It is important to stress that the amplitude of the fluctuations is significantly reduced ($\ll e^2/h$), which is in agreement with the experimental results where the oscillations in the resistance had a typical magnitude of only several Ω .

The above analysis sets the phase coherence length in the dot⁵ to $l_\phi \approx 0.8L = 2 \mu\text{m}$. This value is consistent with the

results^{11,12} but significantly lower than those for the devices studied in Refs. 13 and 14. However, it is worth to stress that different models of determination of l_ϕ give values that can disagree as much as in the order of the magnitude even for the same dot.¹² On the other hand, the above analysis pro-

vides a direct assessment of l_ϕ through specific trajectories of the ballistic billiard.

We thank K.-F. Berggren, J. Martorell, K. Ensslin, and A. S. Sachrajda for valuable discussions. This work was supported by NGSSC and NFR.

¹For a review, see, e.g., C. W. J. Beenakker, *Rev. Mod. Phys.* **69**, 731 (1997).

²M. Brack and R. K. Bhaduri, *Semiclassical Physics* (Addison-Wesley, Reading, MA, 1997).

³C. M. Marcus *et al.*, *Phys. Rev. Lett.* **69**, 506 (1992); A. M. Chang *et al.*, *ibid.* **73**, 2111 (1994); J. P. Bird *et al.*, *Europhys. Lett.* **35**, 529 (1996); Y. Lee *et al.*, *Phys. Rev. B* **56**, 9805 (1997); L. Christensson *et al.*, *ibid.* **57**, 12 306 (1998); P. Bøggild *et al.*, *ibid.* **57**, 15 408 (1998); I. V. Zozoulenko *et al.*, *ibid.* **558**, 10 597 (1998).

⁴M. Persson *et al.*, *Phys. Rev. B* **52**, 8921 (1995); K.-F. Berggren, Z.-L. Ji, and T. Lundberg, *ibid.* **54**, 11 612 (1996).

⁵I. V. Zozoulenko *et al.*, *Phys. Rev. B* **55**, R10 209 (1997).

⁶I. V. Zozoulenko and K.-F. Berggren, *Phys. Rev. B* **56**, 6931 (1997).

⁷C. D. Schwieters, J. A. Alford, and J. B. Delos, *Phys. Rev. B* **54**, 10 652 (1996).

⁸L. Wirtz, J.-Z. Tang, and J. Burgdörfer, *Phys. Rev. B* **56**, 7589

(1997).

⁹W. H. Miller, *Adv. Chem. Phys.* **25**, 69 (1974); R. A. Jalabert, H. U. Baranger, and A. D. Stone, *Phys. Rev. Lett.* **65**, 2442 (1990).

¹⁰See, e.g., S. Datta, *Electronic Transport in Mesoscopic Systems* (Cambridge University Press, Cambridge, 1995).

¹¹H. Hiramoto *et al.*, *Appl. Phys. Lett.* **54**, 2103 (1989); K.-M. H. Lenssen *et al.*, *Phys. Rev. Lett.* **74**, 454 (1995); J. A. Katine *et al.*, *Phys. Rev. B* **57**, 1698 (1998).

¹²Y. Okubo *et al.*, *Phys. Rev. B* **55**, 1368 (1997); P. Bøggild, Ph. D. thesis, Niels Bohr Institute, Copenhagen, 1998.

¹³A. Yacoby *et al.*, *Semicond. Sci. Technol.* **9**, 907 (1994).

¹⁴J. P. Bird *et al.*, *Phys. Rev. B* **51**, 18 037 (1995); R. M. Clarke *et al.*, *ibid.* **52**, 2656 (1995); A. G. Huibers *et al.*, *Phys. Rev. Lett.* **81**, 1917 (1998).

¹⁵I. V. Zozoulenko, F. A. Maaß, and E. H. Hauge, *Phys. Rev. B* **53**, 7975 (1996); **53**, 7987 (1996).

¹⁶H. Ishio, *J. Stat. Phys.* **83**, 203 (1996).